

Giant terahertz pulling force within an evanescent field propelled by wave coupling into radiation and bound modes

Hernán Ferrari^{1,2}

Carlos J. Zapata-Rodríguez³

Mauro Cuevas^{1,2}

¹ Consejo Nacional de Investigaciones Científicas y Técnicas (CONICET)

² Facultad de Ingeniería-LIDTUA-CIC, Universidad Austral, Mariano Acosta 1611, Pilar 1629, Buenos Aires, Argentina.

³ Department of Optics and Optometry and Vision Sciences, University of Valencia, Dr. Moliner 50, Burjassot 46100, Spain.

E-mail: mcuevas@austral.edu.ar

Abstract. Manipulation of subwavelength objects by engineering the electromagnetic waves in the environment medium is pivotal for several particle handling techniques. In this letter, we theoretically demonstrate the possibility of engineering a compact and tunable plasmon-based terahertz tweezer using a graphene monolayer that is deposited on a high-index substrate. Under total-internal-reflection illumination, such device is shown to be capable of inducing an enhanced rotating polarizability thus enabling directional near-field coupling into the graphene plasmon mode and radiation modes in the substrate. As a result of the total momentum conservation, the net force exerted on the particle points in a direction opposite to the pushing force of the exciting evanescent field. Our results can contribute to novel realizations of photonic devices based on polarization dependent interactions between nanoparticles and electromagnetic mode fields.

PACS numbers: 81.05.ue,73.20.Mf,78.68.+m,42.50.Pq

Keywords: Pulling force, graphene, surface plasmons, rotating polarizability, asymmetric modes excitation

A well known property of light-matter interactions is their capacity to manipulate micro and nano particles controlling their state of motion or confine them stable in space [1, 2]. Many configurations containing optical elements have been specially designed for optical trapping, for controlling the rotation of trapped objects, fusion of airborne droplets and optical chromatography [3].

Near-field optics, that is founded in electromagnetic fields existing in the close vicinity of interfaces and whose spatial variation is not constrained by the diffraction limit, have found application in experiments requiring the control of the nano particle positions. Most of the literature in this field has been devoted to configurations that use the total internal reflection (TIR) phenomenon to generate evanescent waves emerging amplified with respect to the incident wave and taking spatial periodicities less than those of the incident photons [4, 5, 6]. In those applications requiring smaller spatial variations, the evanescent wave generated is used to excite surface plasmons (SPs) along a metallic interface near which the particle or an ensemble of particles are placed [7, 8, 9, 10].

In recent years, great efforts have been invested in the development of structures capable to shift to the THz spectrum the optical phenomena taking place in the visible region. Consequently, new materials with novel optical properties in the THz range have found applications. One of the outstanding examples is graphene, a monolayer of carbon atoms arranged in a hexagonal lattice. Thanks to the van der Waals force, a graphene sheet growing by CVD (chemical vapor deposition) method can be tightly coated on the surface of a PMMA material [11]. This surface material has two attractive electromagnetic properties: its transparency and its capacity to support the propagation of SPs on the electromagnetic spectrum from microwaves to THz. These properties have been exploited to enhance the spontaneous emission and the electromagnetic energy transfer, as quantum nanophotonic probes [12], as low frequency photodetectors [13], PT-symmetric plasmonic waveguides [14, 15], resonant cavities and micro antennas to enhance their sensor applications in the THz region [16]. In the framework of optical forces, recently, graphene have been proposed for THz plasmonic nanotrapping [17, 18, 19, 20, 21] and for THz binding of nanoparticles [22].

In the present work we show how the two above mentioned outstanding graphene properties: transparency and plasmonic behavior, can be used to boost THz pulling forces. A highlighted property of the optical pulling force is the fact that its action direction is opposed to the incident pushing force. Since its discovery, about 10 years ago, this counter intuitive feature has attracted the attention of the scientific community and novel designed light structures providing optical pulling force has been realized (see [23] and Ref. therein). Here we propose the first transparent graphene structure demonstrating optical pulling force in the THz spectrum. The mechanism involved in such optical phenomenon takes advantage on two properties: the asymmetric near field pattern produced by an elliptically polarized dipole induced on the particle beyond the critical angle of TIR, and the graphene bound mode excitation along the interface where the particle is nearly placed. Momentum transfer into radiation modes in the dielectric

substrate also contributes in the resulting pulling force.

Let us consider a single plane interface separating two dielectric media. The semi-space $z < 0$ is filled with a dense material of permittivity $\varepsilon_2 = 2.5$ (PMMA, polymethyl methacrylate) and the semi-space $z > 0$ is filled with a less dense medium of permittivity ε_1 (vacuum, $\varepsilon_1 = 1$). A graphene sheet is placed along the plane $z = 0$ which is used to effectively produce the optical pulling force. Since the plasmonic behavior of highly doped graphene is the source of the pulling force intensification, and the fact that only p polarized SPs can be effectively excited in the THz range, in all the examples presented here, the illumination is accomplished by a p polarized plane wave (electric field lying on the plane of incidence) impinging on the interface $z = 0$ with an angle of incidence ϕ from the z axis, with angular frequency ω and amplitude E_{inc} .

In Figure 1 we plotted the square modulus of the electric field at the particle position, $z_0 = 1\mu\text{m}$, as a function of the angle of incidence ϕ . We observe that for incident angles lower than the critical angle $\phi_{crit} = \arcsin(n_1/n_2)$ ($\phi_{crit} \approx 40^\circ$), the $|E|^2$ values for the cases with and without graphene almost coincide. However, for $\phi > \phi_{crit}$, in particular for $\phi_{crit} < \phi < 60^\circ$, the square modulus of the electric field for graphene case is approximately 1.25 times greater than the corresponding value for the case without graphene. From the inset in Figure 1 we see the dependence of the $|E|^2$ intensity as a function of ϕ and the particle position z_0 for $1 < z_0 < 10\mu\text{m}$.

Taking into account that the optical force is proportional to the electric field modulus (and their spatial derivative), a fact that motivated applications of enhanced evanescent fields at dielectric or metallic boundaries for increasing the optical force [9, 24], one intuitively expect that the optical force exerted on the particle in the two structures, with and without graphene are comparable, or at most, does not differ too much. Here we reveal that, in contrast to this expectation, this is not the case. We find that the inclusion of graphene provides a strong interaction between the nanoparticle and the interface giving rise to a pulling force along the flat surface (x direction) reaching values that are at least the same order of magnitude than that of the pushing force produced by the enhanced evanescent field.

In order to find the value of the force acting on the nanoparticle along the x axis, we apply the Green tensor approach by assuming that the size of the particle is lower than photon and plasmon wavelengths, $R \ll \lambda_{sp} \approx \lambda/3$ (the photon wavevector modulus $\lambda = 2\pi c/\omega$). In this framework, the time average of the total force acting on a single particle is written as [6],

$$F_x(\mathbf{r}_0) = \frac{1}{2} \text{Re} \sum_{j=x,y,z} p_j^* \frac{\partial}{\partial x} E_j(\mathbf{r})|_{\mathbf{r}=\mathbf{r}_0}, \quad (1)$$

where E_j is the j component of the electric field, \mathbf{p} is the induced electric dipole on particle at \mathbf{r} position. Taking into account that the electric field in medium 1 can be written as superposition of the electric field in absence of the particle plus the field scattered by the particle, $\mathbf{E}(\mathbf{r}) = \mathbf{E}^{(1)}(\mathbf{r}) + \frac{k_0^2}{\varepsilon_0} \hat{\mathbf{G}}(\mathbf{r}, \mathbf{r}_0) \mathbf{p}$ ($\hat{\mathbf{G}}$ is the Green tensor of the

structure), we obtain $F_x(\mathbf{r}_0) = F_0(\mathbf{r}_0) + F_s(\mathbf{r}_0)$, where

$$F_0 = \frac{1}{2}k_x \left(\text{Im}(\hat{\alpha}_{xx})|\mathbf{E}_x^{(1)}|^2 + \text{Im}(\hat{\alpha}_{zz})|\mathbf{E}_z^{(1)}|^2 \right) \quad (2)$$

is the x component of the force due to the enhanced evanescent electric field in medium 1, and

$$F_s = -\frac{k_0^2}{\varepsilon_0} \text{Im} \left(\frac{\partial}{\partial x} G_{s,xz}(\mathbf{r}_0, \mathbf{r})|_{\mathbf{r}=\mathbf{r}_0} \right) \text{Im}(\hat{\alpha}_{xx}^* \hat{\alpha}_{zz} \mathbf{E}_x^{(1)*} \mathbf{E}_z^{(1)}) \quad (3)$$

is the x component of the force due to the interaction between the induced dipole moments and the interface, and $\hat{\alpha}$ is the particle polarizability taking into account the interaction with the interface [25].

Figure 2 shows the terahertz force normalized with respect to the radiation force from the incident plane wave of the same amplitude as in Figure 1 acting on the same particle in vacuum $F_{inc} = \frac{1}{2}k_0 \text{Im}\alpha_0 |\mathbf{E}_{inc}|^2$, *i.e.*, $f_0 = F_0/F_{inc}$, $f_s = F_s/F_{inc}$, $f_x = f_0 + f_s$. From Figure 2a (without graphene), we observe that the curve for the force f_0 has the same shape as that corresponding to $|E|^2$ in Figure 1. We also observe that the total force f_x is reduced with respect to f_0 because the f_s component is negative, *i.e.*, f_s is in opposite direction as that of f_0 . This fact arise from the transmitted power into medium 2 beyond the critical angle of TIR (see supplementary information S2).

In Figure 2b we plotted the force curves when the substrate is covered with graphene. As in the above case, the shape of the f_0 curve coincides with that of the enhanced evanescent field in Figure 1. However, the values of f_0 in Figure 2b result amplified in a factor $\approx 25 - 30$ with respect to those plotted in Figure 2a. This is true because two reasons. The first one is related with the ratio between the fields $|E|^2$ for the cases with and without graphene, which provides a factor ≈ 1.25 (see curves in Figure 1), and the second one (the more important contribution) is related to the polarizability modifications (mainly in the imaginary part) due to self-action effect of the particle through the graphene interface. These increments are: $\text{Im}\alpha_{xx} \approx 25\text{Im}\alpha_0$ and $\text{Im}\alpha_{zz} \approx 60\alpha_0$ (see supplementary information S2). On the other hand, for the case without graphene, the increments are: $\text{Im}\alpha_{xx} \approx 1.2\text{Im}\alpha_0$ and $\text{Im}\alpha_{zz} \approx 2.4\alpha_0$. Therefore, a rough estimation of the ratio between the values of f_0 for the cases with and without graphene gives $1.25 \times (25 + 60)/(1.2 + 2.4) \approx 30$.

In addition, the force component f_s is two orders of magnitude higher than that corresponding to the case without graphene. As a result, the total force f_x results negative (in the $-x$ direction) for angles of incidence $\phi > 41^\circ$, *i.e.*, an improved pulling force is acting on the particle.

To find the underlying physical mechanism of the emerging pulling force, we extract the SP contribution to the F_s force (3) (see supporting information S1),

$$F_{sp} \approx -\frac{|\alpha_0|^2 |t|^2 |E_{inc}|^2 \varepsilon_2^{3/2} \sin \phi \kappa}{4\varepsilon_0 \varepsilon_1^3 (\varepsilon_1 + \varepsilon_2)} k_{sp}^4 \times e^{-2(k_0 \kappa + k_{sp})z_0}, \quad (4)$$

where α_0 is the particle polarizability in vacuum, k_{sp} is the propagation constant of SPs, $\kappa = \sqrt{\varepsilon_2 \sin^2 \phi - \varepsilon_1}$ and E_{inc} is the amplitude of the incident electric field. Note

that we have used the fact that $\alpha_{xx}^* \alpha_{zz} \approx |\alpha_0|^2$ (see supplementary information S2). In Figure 2 we observe that this force almost coincide with F_s given by Eq. (3). We attribute the small difference between F_s and F_{sp} to the contribution of radiative modes into medium 2 under TIR (see inset at below in Figure 2 which shows the radiation pattern for $\phi > \phi_{crit}$). As the contrast between media 1 and 2 increases, the asymmetric radiation pattern and, consequently, the contribution of radiation modes to the pulling force becomes more evident (see supplementary information S3).

We emphasize that the origin of the F_{sp} does not arise on the SP excitation along graphene by plane wave incidence, as in attenuated total reflection devices [7]. Instead of this, the origin of F_{sp} is due to the interaction between the elliptically dipole moment induced on the particle by the evanescent field and SPs on graphene. Explicitly, the evanescent field $\mathbf{E}^{(1)} \approx [i\kappa \hat{x} - \sqrt{\varepsilon_2} \sin \phi \hat{z}]$, $\phi > \phi_{crit}$, induces a dipole moment $\mathbf{p} \approx \alpha_0 \mathbf{E}^{(1)}$ where the phase difference between the x and z components is equal to $-\pi/2$. Thus, the near field scattered by this rotating dipole excites SPs and radiation modes into the substrate with an anisotropic spatial distribution, this being more intense for $+x$ direction than for $-x$ direction (see inset in Figure 2b). As a result of the momentum conservation, a force on the particle in the $-x$ direction appears. In virtue of the mirror symmetry respect to the $x = 0$ plane, if $\phi < 0$ then the phase difference between the components x and z of the induced dipole turns to $+\pi/2$, leading to a graphene SP excitation and associated force with reversed directionality. In this framework and based on the fact that a linear polarization can be decomposed as two circular polarized with opposed spins, one would think that below TIR ($|\phi| < \phi_{crit}$) for which the dipole moment excited on the nanoparticle has linear polarization, an isotropic SP spatial distribution results (see inset in Figure 2b). As a consequence, a net null F_{sp} force results.

A pulling force assisted by SPs has also been reported in [25] for metallic plane interfaces. However, the mechanism rising the pulling force in the system here presented differs from that reported in [25]. While in that work the interference of the incident and reflected fields on an impenetrable interface provides the necessary asymmetric excitation of SPs, in our system TIR condition is required at a transparent material interface to reach the asymmetric excitation of SPs enabling the pulling force.

Figure 3 shows the normalized force f_x as a function of the angle of incidence and the distance z_0 from the interface. We observe two well defined regions: one of them, the blue zone, corresponding to points (ϕ, z_0) where the force is positive and another zone, the red zone, where the force is negative. For all angles of incidence, we note a maximum value of z_0 from which the total force is positive. This occurs because the force F_s is greater than F_0 near the graphene interface and, in addition, F_s decays much faster than F_0 . This fact can be understood from Eqs. (2) and (4) where we see that $F_0 \approx \exp(-2k_0\kappa z_0)$ and $F_s \approx \exp(-2[k_{sp} + k_0\kappa]z_0)$. Therefore, the decay distances for F_0 and F_s are $\delta_0 \approx 1/(2k_0\kappa)$ and $\delta_s \approx 1/(2[k_{sp} + k_0\kappa])$, respectively. As a consequence $\delta_0 > \delta_s$. For instance, for angles of incidence near the critical angle, *i.e.*, $\sin \phi \approx \sqrt{\varepsilon_1/\varepsilon_2}$, $\delta_0 \rightarrow \infty$, which mean that the force F_0 almost does not decay with z_0 , and $\delta_s \approx 3\mu\text{m}$.

In conclusion, we have revealed a novel form for generating a pulling force within an evanescent field by near-field directional coupling into multiple photonic channels. In the THz spectrum, such particle handling mechanism is enabled by a simple graphene structure lying on a high-index substrate. The net pulling force is achieved through the strong field scattered by particle illumination under total-internal-reflection conditions. The magnitude of this pulling force results from the superposition of two processes: one of them provided by the interaction between the particle and the plasmon field scattered back to the particle site, and the other one driven by asymmetric excitation of forbidden propagation modes into the substrate [26]. Both phenomena can be considered as a manifestation of the interaction between a rotating dipole moment and the vectorial modes of an electromagnetic structure [27, 28]. Our theoretical analysis is carried out by using the Green tensor approach. We provide analytical expressions revealing the characteristics of the SP force, which is the dominant source of the pulling force, with dependence upon geometrical and constitutive parameters.

Acknowledgments

The authors acknowledge the financial supports of Universidad Austral O04-INV0 0 020 and Consejo Nacional de Investigaciones Científicas y Técnicas (CONICET). Discussions with Prof. Francisco Ibanez (Laboratorio de Nanoscopias y Fisicoquímica de Superficies, INIFTA, CONICET, Argentina) about CVD method and the transferring protocol involving the use of PMMA are gratefully acknowledged.

Disclosures

The authors declare no conflicts of interest.

- [1] Ashkin, A., Acceleration and trapping of particles by radiation pressure. *Phys. Rev. Lett.* 24, 156-159 (1970).
- [2] Ashkin, A., Dziedzic, J. M., Bjorkholm, J. E. and Chu, S., Observation of a single beam gradient force optical trap for dielectric particles. *Opt. Lett.* 11, 288-290 (1986).
- [3] A Jonas, P Zemanek, Light at work: The use of optical forces for particle manipulation, sorting, and analysis, *Electrophoresis* 29, 4813-4851 (2008)
- [4] S. Kawata and T. Sugiura, *Opt. Lett.* 17, 772 (1992).
- [5] Ma. Lester and M. Nieto-Vesperinas, Optical forces on microparticles in an evanescent laser field, *OPTICS LETTERS* 24, (1999).
- [6] PC Chaumet, and M Nieto-Vesperinas, "Optical binding of particles with or without the presence of a flat dielectric surface," *Phys. Rev. B* 64, 035422 (2001).
- [7] Y G Song, B M Han, S Chang, Force of surface plasmon-coupled evanescent fields on Mie particles, *Optics Communications* 198, 7-19 (2001).
- [8] G Volpe, R Quidant, G Badenes, and D Petrov, Surface Plasmon Radiation Forces, *PHYSICAL REVIEW LETTERS* 96, 238101 (2006).
- [9] O M Marago, P. H. Jones, P. G. Gucciardi, G. Volpe and A. C. Ferrari, Optical trapping and manipulation of nanostructures, *NATURE NANOTECHNOLOGY* 8, (2013)
- [10] M. L. Juan, M. Righini and R. Quidant, Plasmon nano-optical tweezers, *Nature Photonics* 5, (2011)

- [11] Dalfovo, M. C., Lacconi, G., Moreno, M., Yappert, M. C., Sumanasekera, G. U., Salvarezza, R. C., F. J. Ibanez, Synergy between Graphene and Au Nanoparticles (Heterojunction) towards Quenching, Improving Raman Signal, and UV Light Sensing, ACS Applied materials and interfaces, (2014) 6384-6391.
- [12] PAD Gonçães, Thomas Christensen, Nuno MR Peres, Antti-Pekka Jauho, Itai Epstein, Frank HL Koppens, Marin Soljacic, N Asger Mortensen, Nature Communications 12, (2021), 3271
- [13] Y. Ding, Z. Cheng, X. Zhu, K. Yvind, J. Dong, M. Galili, H. Hu, N. A. Mortensen, S. Xiao, L. K. Oxenløwe, Ultra-compact graphene plasmonic photodetector with the bandwidth over 110GHz, Nanophotonics 9, (2020) 317-325.
- [14] X. Lin, R. Li, F. Gao, E. Li, X. Zhang, B. Zhang, and H. Chen, Loss induced amplification of graphene plasmons, Opt. Lett. 41(4), 681-684 (2016).
- [15] Y. Fan, N.-H. Shen, F. Zhang, Q. Zhao, H. Wu, Q. Fu, Z. Wei, H. Li, and C. M. Soukoulis, Graphene plasmonics: a platform for 2d optics, Adv. Opt. Mater. 7(3), 1800537 (2019).
- [16] R. Filter, M. Farhat, M. Steglich, R. Alaee, R. Rockstuhl and F. Lederer, "Tunable graphene antennas for selective enhancement of THz-emission," Opt. Express, 21 (2013), p. 3737, (2020).
- [17] P. Q. Liu and P. Paul, "Graphene Nanoribbon Plasmonic Conveyor Belt Network for Optical Trapping and Transportation of Nanoparticles," ACS Photonics 7, (2020) 3456–3466
- [18] Zi Shen, M. Becton, D. Han, X. Fang, X. Wang, L. Zhang, and X. Chen, "Terahertz plasmonic nanotrapping with graphene coaxial apertures," Phys. Rev. A 102, 053507 (2020).
- [19] M. Samadi, S. Darbari and M. K. Moravvej-Farshi, "Numerical Investigation of Tunable Plasmonic Tweezers based on Graphene Stripes," Sci. Rep. 7 14533 (2017)
- [20] A. F. da Mota, A. Martins, J. Weiner, P. Courteille, E. R. Martins, and B. V. Borges, "Design and analysis of nanopatterned graphene-based structures for trapping applications," Phys. Rev. B 102, 085415 (2020)
- [21] H. Chen, Y. Huang, "Tunable optical force on nonlinear graphene-wrapped nanoparticles," Phys. Lett. A 384 (2020) 126733
- [22] H. Ferrari, C. J. Zapata-Rodríguez and M. Cuevas, "Terahertz binding of nanoparticles based on graphene surface plasmon excitations," Journal of Quantitative Spectroscopy and Radiative Transfer 278, 108009 (2022).
- [23] W. Ding, To. Zhu, L. M. Zhou, and C. W. Qiu, "Photonic tractor beams: a review," Advances Photonics 1, 024001, (2019).
- [24] Do Gao, W. Ding, M. Nieto-Vesperinas, X. Ding, M. Rahman, T. Zhang, C. Lim and C-W Qiu, Optical manipulation from the microscale to the nanoscale: fundamentals, advances and prospects, Light: Science and Applications 6, e17039 (2017).
- [25] M. I. Petrov, S. V. Sukhov, A. A. Bogdanov, A. S. Shalin, A. Dogariu, Surface plasmon polariton assisted optical pulling force, Laser Photonics Rev. 10, 116-122 (2016).
- [26] L. Novotny. Allowed and forbidden light in near-field optics. II. Interacting dipolar particles. JOSA A, 14(1), (1997) 105-113.
- [27] F. J. Rodríguez-Fortuno, G. Marino, P Ginzburg, D. O'Connor, A. Martinez, G. A. Wurtzand, A. V. Zayatz, "Near-Field Interference for the Unidirectional Excitation of Electromagnetic Guided Modes," Science 340, (2013).
- [28] M. Neugebauer, T. Bauer, A. Aiello and P. Banzer, Measuring the Transverse Spin Density of Light, Phys. Rev. Lett. 114, 063901 (2015).

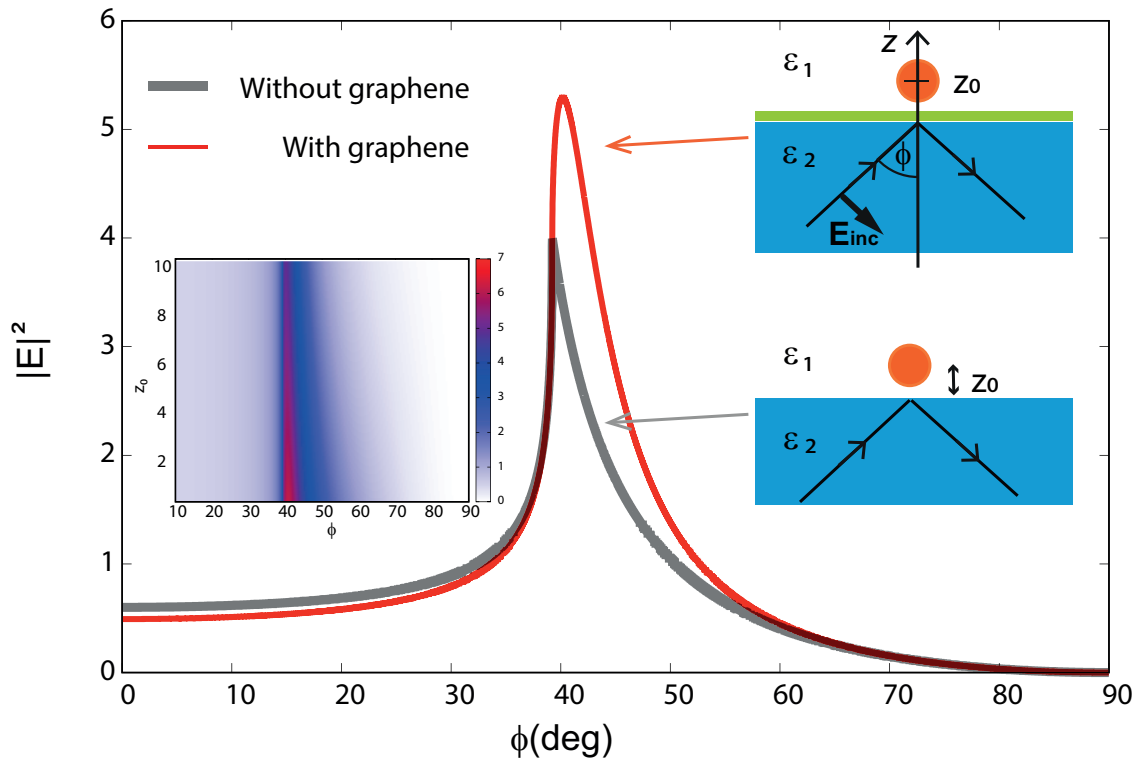


Figure 1. Square modulus of the electric field (in arbitrary units) at the particle position $z_0 = 1\mu\text{m}$ for two cases: with and without graphene as illustrated in the insets on the right. The permittivity of medium 1 and 2 is $\epsilon_1 = 1$ and $\epsilon_2 = 2.5$, respectively. Wavenumber of the incident field is $\omega/c = 0.05\mu\text{m}^{-1}$ ($\lambda \approx 126\mu\text{m}$) and the graphene parameters are $T = 295\text{K}$, $\mu_c = 0.4\text{eV}$ and $\gamma_c = 0.1\text{meV}$. Inset: Square modulus of the electric field at the particle position z_0 ($1 < z_0 < 10\mu\text{m}$) and angle of incidence ϕ ($0 < \phi < 90^\circ$).

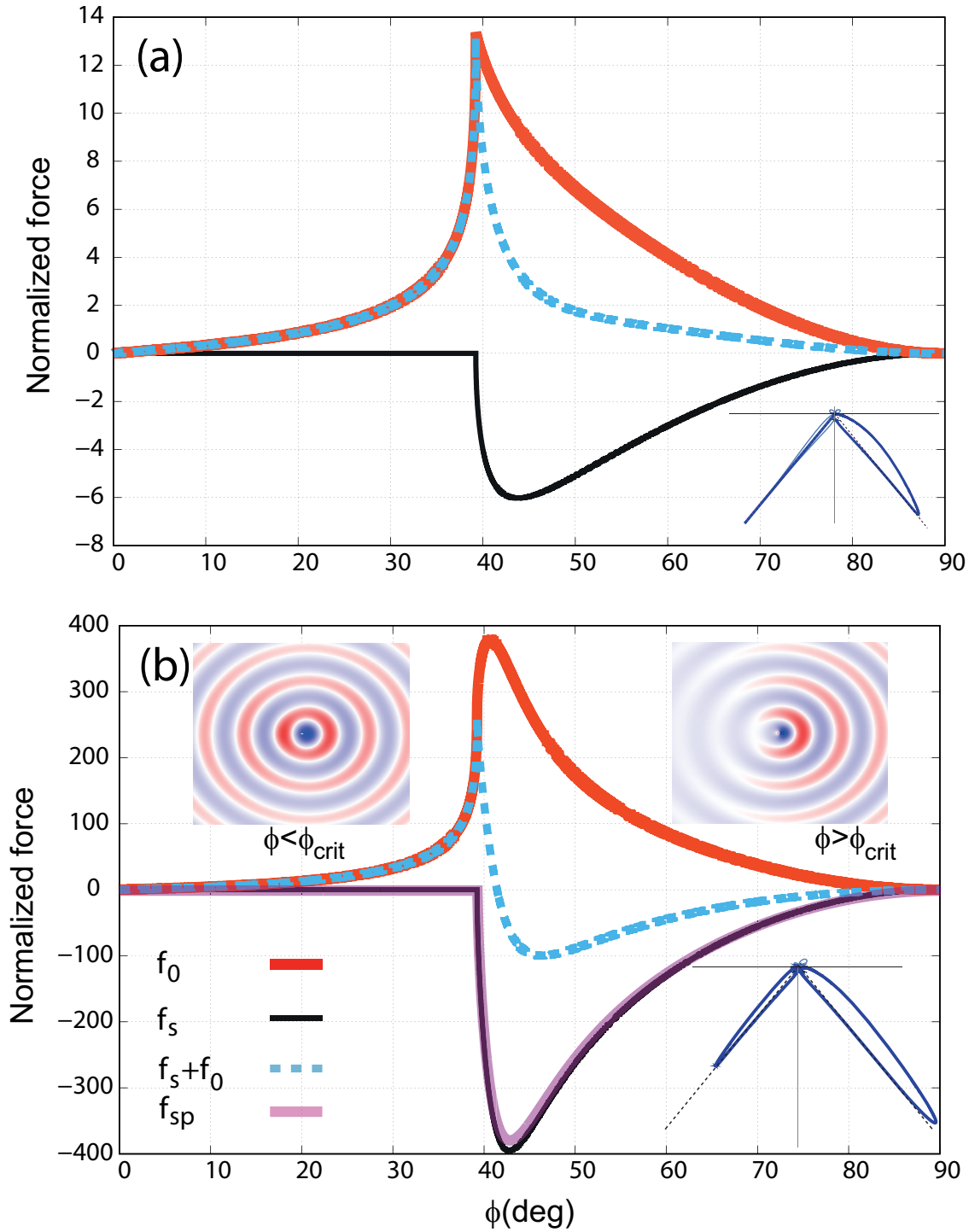


Figure 2. THz force normalized with respect to the radiation force F_{inc} along the x axis as a function of the angle of incidence for the case in which the interface has not graphene (a), and the case in which the interface is composed of graphene (b). The graphene parameters are $T = 295\text{K}$, $\mu_c = 0.4\text{eV}$ and $\gamma_c = 0.1\text{meV}$. The particle (radius $R = 0.045\mu\text{m}$ and permittivity $\epsilon_p = 3.9$) is placed at distance $1\mu\text{m}$ from the interface ($z_0 = 1\mu\text{m}$). Inset in (b) shows the spatial distribution of the z component of the electric field along graphene for angles of incidence higher (right) and lower (left) than the critical angle of total reflection, respectively.

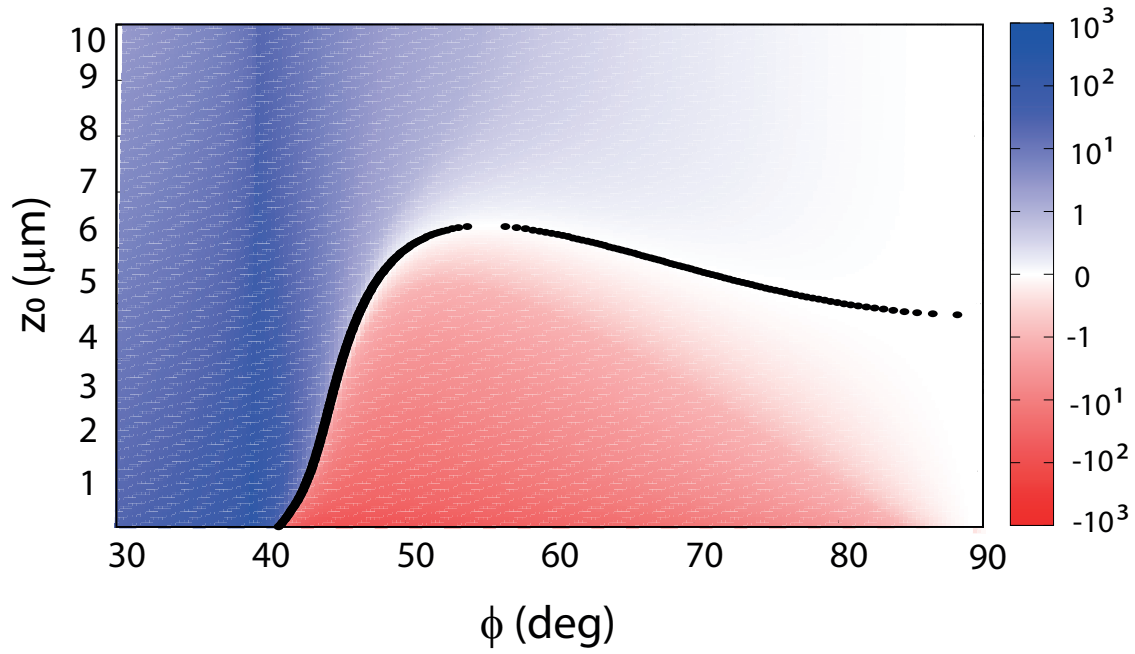


Figure 3. Normalized THz force f_x as a function of the angle of incidence ϕ and the z_0 distance. Red, negative values, blue, positive values. Black dot corresponds to points (ϕ, z_0) for which the total force $f_x = 0$. All other parameters are the same as in Figure 2b.